

A NEW NUMERICAL MODEL FOR THE PUMP-TO-SIGNAL RIN TRANSFER IN SINGLE-PUMP FIBER OPTICAL PARAMETRIC AMPLIFIERS*

H. PAKARZADEH AND A. ZAKERY**

Department of Physics, College of Sciences, Shiraz University, Shiraz, I. R. of Iran
Email: zakery@physics.susc.ac.ir

Abstract – Using a new numerical model, the pump-to-signal relative intensity noise (RIN) transfer in single-pump fiber optical parametric amplifiers for low modulation frequencies is investigated. The model includes fiber loss, pump depletion, as well as the gain saturation, and therefore, it can describe the practical circumstances associated with various applications of fiber optical parametric amplifiers. The nonlinear dynamics of the RIN transfer for different pump and signal powers is studied. The impact of the input pump and signal powers and signal wavelength on the RIN transfer is also investigated. Finally, the model is compared to the available experimental data and a very good agreement is obtained.

Keywords – Parametric amplification, relative intensity noise (RIN), optical fiber

1. INTRODUCTION

Fiber optical parametric amplifiers (FOPAs) have attracted significant research interest in recent years, since they hold great promise for several applications including high-gain amplification [1], wavelength conversion [2], regeneration [3], all-optical sampling [4] and wide-bandwidth amplification [5].

One of the main concerns in optical communications is the noise figure (NF) and its detrimental effects on device performance. Due to the extremely fast response time of the refractive index and power-dependent parametric gain, any pump fluctuation is easily transferred to the amplified signal or the generated idler. As a result, noise in FOPAs is dominated by the transfer of relative intensity noise (RIN) associated with the pump laser which can considerably degrade the FOPA. For example, it is well known that in an ideal phase-insensitive FOPA, the minimum achievable NF in the quantum limit is 3dB [6]. However, in practical systems with moderately high gains and high input signal powers, RIN in the pump keeps the NF above the quantum limit. Some sources that introduce RIN into the pump are: 1) stimulated Brillouin scattering (SBS) suppression done by either phase modulation or by frequency modulation of the laser diode, 2) amplification of the pump wave by erbium-doped fiber amplifiers (EDFAs), 3) RIN due to the pump itself. RIN from all these sources leads to a variation of the parametric gain, which finally impairs the performance of FOPAs.

Several studies on noise characteristics of FOPAs have been reported from different perspectives including its dependency on: gain and wavelength [7], dispersion fluctuations [8], optical signal to noise ratio of the pump [9], pump noise [10], and Raman effect [11]. Nonetheless, very little attention has been paid directly to the pump-to-signal RIN transfer in FOPAs. M.E. Marhic, et al, have investigated the transfer of low-frequency intensity modulation of the pump to the signal and derived analytical expressions [12]. As can be seen, most of the works that have been done in the context of noise in FOPAs date back to some years ago, however, quite recently some other aspects of noise in single-pump FOPAs

*Received by the editor December 19, 2010 and in final revised form March 13, 2011

**Corresponding author

have been also studied [13, 14]. This shows that the noise in FOPAs is still attractive for the scientific community.

In almost all the above works, the main focus is on the experimental side, and all the theories that have been used in these works are valid under some approximations including a lossless and/or undepleted FOPA. To develop a theory which covers the experimental conditions, one has to take into account the losses as well as the pump depletion. The role of losses is important when the fiber is too long or the coupling and/or the distributed losses are not negligible [15]. Inclusion of the pump depletion must be considered if one plans to investigate the RIN transfer in a FOPA which employs high signals or operates near the saturation.

In this paper, a comprehensive numerical model for investigating the pump-to-signal RIN transfer in single-pump FOPAs is presented. The model predicts RIN transfer when the modulation frequencies are low and includes losses, pump depletion, and gain saturation. We also investigate the dependency of the RIN transfer on the input signal and pump powers, signal wavelength, as well as on the fiber length. Our numerical method yields results which match very well with the analytical ones whenever a lossless fiber and a very weak signal are assumed. Moreover, it can describe other practical circumstances in some applications like: efficient wavelength conversion where the pump depletion cannot be ignored, and also in regenerators and amplitude limiters [3, 16, 17] where the FOPA works in the saturation regime. Indeed, for these applications the analytical solutions no longer work and one has to use a sophisticated model to cover the practical circumstances. The method is also faster than solving the full generalized nonlinear Schrodinger equation (NLSE). To our knowledge this is the first time that such a simple, fast and comprehensive method for investigating the pump-to-signal RIN transfer in single-pump FOPAs is presented.

The paper is organized as follows: In section 2 an efficient numerical model for the calculation of RIN transfer in single-pump FOPAs under the low-modulation frequency regime is developed. In the next section, the simulation results carried out for several operating conditions are presented in two parts: Part 3.1 which is purely devoted to the numerical results with a focus on nonlinear dynamics of the RIN transfer, and its dependency on some parameters like input pump and signal powers as well as when the FOPA saturates; and Part 3.2 in which the numerical results are compared to the experiments and the theory of ref. 12. Finally, in Section 4, the basic conclusions reached are summarized.

2. THEORY

We start with the well-known coupled amplitude equations governing the evolution of the pump, signal and idler in a CW single-pump FOPA [18, 19]:

$$\frac{\partial A_p}{\partial z} = i\gamma \left(|A_p|^2 + 2|A_s|^2 + 2|A_i|^2 \right) A_p + 2i\gamma A_s A_i A_p^* \exp(i\Delta\beta z) - \frac{1}{2}\alpha A_p \quad (1)$$

$$\frac{\partial A_s}{\partial z} = i\gamma \left(|A_s|^2 + 2|A_i|^2 + 2|A_p|^2 \right) A_s + i\gamma A_i^* A_p^2 \exp(-i\Delta\beta z) - \frac{1}{2}\alpha A_s \quad (2)$$

$$\frac{\partial A_i}{\partial z} = i\gamma \left(|A_i|^2 + 2|A_s|^2 + 2|A_p|^2 \right) A_i + i\gamma A_s^* A_p^2 \exp(-i\Delta\beta z) - \frac{1}{2}\alpha A_i \quad (3)$$

where A_p , A_s , and A_i are the amplitudes of the pump, signal, and idler waves respectively, γ is the nonlinear coefficient, and α is the fiber loss. $\Delta\beta = \beta(\omega_s) + \beta(\omega_i) - 2\beta(\omega_p)$ is the linear wave vector mismatch of the interacting waves, and $\beta_{s,i,p}$ is the mode propagation constant of each lightwave calculated at its central frequency.

Since we are going to modulate the intensity of the pump wave at the input of the FOPA with relatively low modulation frequencies, normally less than several GHz, one can assume that the pump varies so slowly such that any explicit time dependency can be safely neglected. Hence, here the usual steady-state expressions are used.

Introducing a noise term on the pump amplitude, as a small sinusoidal perturbation $\Delta A_p(z)$, the pump amplitude can be written as $A_p(z) = \bar{A}_p(z) + \Delta A_p(z)$, where the mean pump amplitude $\bar{A}_p(z)$ is the solution of Eq. (1). Experimentally this corresponds to the modulation of the pump intensity at the input of FOPA using an intensity modulator driven by a sinusoidal radio-frequency (RF) generator. Although intensity modulation (IM) of the pump generally accompanies frequency modulation (FM), in order to simplify the analysis, the initial pump IM is assumed not to be accompanied by FM. Therefore, IM can be considered to be equivalent to amplitude modulation (AM).

Due to the very fast nonlinear interactions, this perturbation can be easily transferred to the signal and idler waves. We denote the resulting amplitude of the signal: $A_s(z) = \bar{A}_s(z) + \Delta A_s(z)$, and of the idler: $A_i(z) = \bar{A}_i(z) + \Delta A_i(z)$, where the mean signal and idler amplitudes $\bar{A}_s(z)$ and $\bar{A}_i(z)$, are the solutions of Eq. (2) and Eq. (3), respectively. By substituting $A_{p,s,i}(z)$ into the Eq. (1)-(3) and assuming $\Delta A_p(z) \ll \bar{A}_p(z)$, $\Delta A_s(z) \ll \bar{A}_s(z)$, and $\Delta A_i(z) \ll \bar{A}_i(z)$, the propagation equations for the pump, signal, and the idler amplitude modulations are respectively given by:

$$\frac{\partial \Delta A_p}{\partial z} = i\gamma \bar{A}_p \left\{ \Delta A_p \bar{A}_p^* + \bar{A}_p \Delta A_p^* + 2 \left(\Delta A_s \bar{A}_s^* + \bar{A}_s \Delta A_s^* + \Delta A_i \bar{A}_i^* + \bar{A}_i \Delta A_i^* \right) \right\} + i\gamma \left(|\bar{A}_p|^2 + 2|\bar{A}_s|^2 + 2|\bar{A}_i|^2 \right) \Delta A_p + 2i\gamma \exp(i\Delta\beta z) \left(\Delta A_s \bar{A}_i \bar{A}_p^* + \bar{A}_s \Delta A_i \bar{A}_p^* + \bar{A}_s \bar{A}_i \Delta A_p^* \right) - \frac{1}{2} \alpha \Delta A_p \quad (4)$$

$$\frac{\partial \Delta A_s}{\partial z} = i\gamma \bar{A}_s \left\{ \Delta A_s \bar{A}_s^* + \bar{A}_s \Delta A_s^* + 2 \left(\Delta A_i \bar{A}_i^* + \bar{A}_i \Delta A_i^* + \Delta A_p \bar{A}_p^* + \bar{A}_p \Delta A_p^* \right) \right\} + i\gamma \left(|\bar{A}_s|^2 + 2|\bar{A}_i|^2 + 2|\bar{A}_p|^2 \right) \Delta A_s + i\gamma \exp(-i\Delta\beta z) \left(\Delta A_i^* \bar{A}_p^2 + 2\bar{A}_i^* \bar{A}_p \Delta A_p \right) - \frac{1}{2} \alpha \Delta A_s \quad (5)$$

$$\frac{\partial \Delta A_i}{\partial z} = i\gamma \bar{A}_i \left\{ \Delta A_i \bar{A}_i^* + \bar{A}_i \Delta A_i^* + 2 \left(\Delta A_s \bar{A}_s^* + \bar{A}_s \Delta A_s^* + \Delta A_p \bar{A}_p^* + \bar{A}_p \Delta A_p^* \right) \right\} + i\gamma \left(|\bar{A}_i|^2 + 2|\bar{A}_s|^2 + 2|\bar{A}_p|^2 \right) \Delta A_i + i\gamma \exp(-i\Delta\beta z) \left(\Delta A_s^* \bar{A}_p^2 + 2\bar{A}_s^* \bar{A}_p \Delta A_p \right) - \frac{1}{2} \alpha \Delta A_i \quad (6)$$

where * denotes the complex conjugate.

The RIN transfer function is defined as $10\log\left(\frac{r_s}{r_p}\right)$, where $r_s = \left(\frac{\Delta P_s}{\bar{P}_s}\right)^2$ is the signal RIN at the output of the FOPA and $r_p = \left(\frac{\Delta P_p}{\bar{P}_p}\right)^2$ is the pump RIN at the input of the FOPA. $\bar{P}_{p,s} = \bar{A}_{p,s} \bar{A}_{p,s}^*$ is the mean value of the pump and signal powers, respectively. $\Delta P_{p,s}$, which is defined through the relation: $\Delta P_{p,s} = \bar{A}_{p,s}^* \Delta A_{p,s} + \bar{A}_{p,s} \Delta A_{p,s}^*$, corresponds to the power variations of the pump and signal waves, respectively.

The state of polarization of all waves is considered to be the same throughout the propagation. To increase the accuracy of the theory, the fiber loss has also been included as it may have an important role for other types of fibers which possess higher loss or for longer lengths of FOPAs. However, as it is very common in the FOPA work, the loss can be assumed to be the same for all three waves, since the wavelengths of the waves are very close to each other. To avoid further complexities, nonlinear coefficients of all waves are also considered to be equal. Finally, by solving six coupled equations, three

for the mean amplitudes and three for the corresponding amplitude variations, RIN transfer in single-pump FOPAs is investigated.

3. RESULTS AND DISCUSSIONS

a) Numerical Results

In this part, we have performed our calculations for a highly nonlinear fiber (HNLF) with $\gamma = 11.5 \text{ W}^{-1} \text{ km}^{-1}$, $\alpha = 0.74 \text{ dB/km}$, and effective mode area $A_{\text{eff}} = 11.7 \text{ } \mu\text{m}^2$. The zero-dispersion wavelength is 1560.5 nm where the dispersion slope is $S = 0.015 \text{ ps}/(\text{nm}^2 \text{ km})$ [3]. The pump and signal wavelengths are assumed 1564 nm and 1546 nm, respectively. Throughout the calculations the input pump RIN is fixed at -100 dB [20]. This means that we assume the intrinsic RIN without an external IM. In order to investigate the pump- to- signal RIN transfer easily, the initial signal is considered to contain no RIN, i.e., $r_s = 0$.

Figure 1 shows the evolution of the RIN transfer along the fiber for various input pump powers. The input signal power is as small as -30 dBm. Each curve describes the nonlinear dynamics of the RIN transfer for a given pump power. As is seen, for higher input pump powers the RIN transfer is higher as well. Since the initial signal RIN is zero and there is slight nonlinear interaction for a very short length, curves start with very low RIN transfers. As the signal propagates along the fiber, it acquires some noise from the pump due to nonlinear interactions until the phase matching is completely fulfilled and the maximum value of the RIN transfer occurs. Then, due to the periodic behavior of the phase matching condition, the RIN transfer goes through its maximum value and finally decreases. This trend is more evident for the bottom curve, where the pump power is the lowest. It should be noted that the phase matching condition for the amplitude variations is not the same as that of mean amplitudes (unmodulated amplitudes). This means that the phase matching condition for the former is modified as is evident from the extra terms which appear on the right-hand side of Eqs. (4)-(6) compared to that of Eqs. (1)-(3). An equivalent explanation could be provided in terms of modulated gain which will be given afterwards.

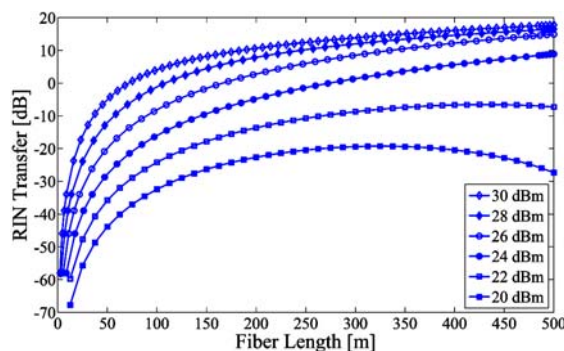


Fig. 1. Evolution of the RIN transfer along the fiber for various input pump powers. $P_s = -30 \text{ dBm}$ and $r_p = -100 \text{ dB}$.

In Fig. 2 the evolution of the RIN transfer along the fiber for various input signal powers is shown. The input pump power is 30 dBm. As the input signal power increases, it depletes the pump power which in turn leads to the reduction of the RIN transfer level. However, since the signal power is relatively low compared to the input pump power, it requires more interaction length in order for the depletion to take place. For higher signal powers FOPA starts to go to saturation where the RIN transfer is minimum. The origin of the periodic behavior refers to the phase matching condition of the parametric process. It means that for a perfect phase matching, the linear wave vector mismatch of the interacting waves must compensate the nonlinear wave vector mismatch of the waves. Therefore, the power always flows from

the pump into the signal until the perfect phase matching is achieved. Beyond the perfect phase matching, however, the reverse process takes place, i.e. the power flows from the signal to the pump. The nonlinear contribution of the phase matching condition is equal to $\gamma P_p z$, and therefore at a lower pump power P_p the phase matching condition is fulfilled at shorter fiber lengths. Since the evolution of the pump power along the fiber depends on the signal power, more pump depletion occurs for higher signal powers and therefore the perfect phase matching is satisfied at shorter fiber lengths. This is why dips in Fig. 2 appear at shorter lengths when the signal powers become high.

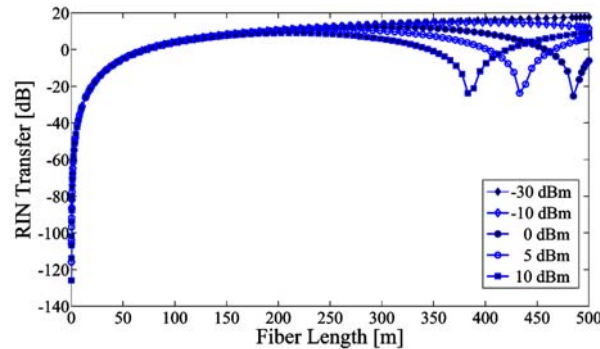


Fig. 2. Evolution of the RIN Transfer along the fiber for various input signal powers. $P_p = 30$ dBm and $r_p = -100$ dB.

Figure 3 shows the evolution of the gain variation due to the modulated pump along the fiber for the same parameters as in Fig. 2. This figure is intended to justify the behavior of curves in Fig. 2. As the pump wave is modulated, the parametric gain is also modulated owing to its power dependency. Therefore, we can write $G = \bar{G} + \Delta G$ where \bar{G} is the unmodulated gain and ΔG is the modulated gain or the gain variation due to the pump modulation. Since the gain definition is $G = P_s(L)/P_s(0)$ where $P_s(L)/P_s(0)$ is the signal power at the output/ input of the FOPA, one can derive the expression for the gain variation as $\Delta G = \Delta P_s(L)/\bar{P}_s(0)$. $\Delta P_s(L)$ represents the signal power variation at the output of the FOPA and $\bar{P}_s(0)$ is the mean signal power at the FOPA input. To derive the expression of gain variation a zero input signal RIN has been assumed. It is interesting to note that Fig. 2 mimics gain variation, and in particular, dips are seen at the same lengths as in Fig. 3. The gain variation is higher for lower signal powers, since at low signal powers the pump depletion is low. In other words, since the pump wave is mainly responsible for the RIN transfer, as we saw explicitly in Fig. 1, the higher pump powers exhibit the higher RIN transfers. On the other hand, as the signal power increases the FOPA reaches its saturation where the gain is robust against the fluctuations [21]. One can also plot a similar figure for the parameters of Fig. 1 in order to verify this fact.

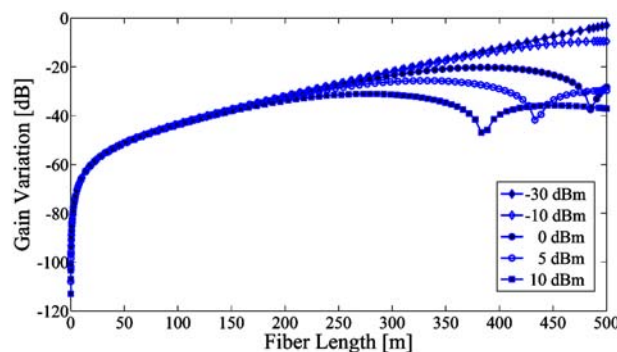


Fig. 3. Evolution of the gain variation due to the modulated pump along the fiber for various input signal powers. $P_p = 30$ dBm and $r_p = -100$ dB.

Figure 4 shows the RIN transfer versus the input signal power for three different input pump powers. The fiber is 500-m long. The figure emphasizes the RIN transfer behavior near the saturation point. As it is known from the saturation behavior of the FOPA, the input signal power at which the parametric gain starts to saturate is increased as the pump power is decreased. A similar feature can also be seen for the RIN transfer where it decreases as the signal power increases such that its minimum is near the saturation point. Again, for the small-signal gain, the higher RIN transfer corresponds to the higher pump power.

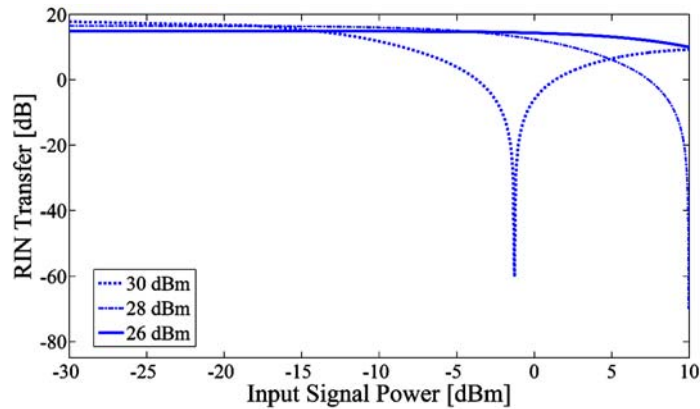


Fig. 4. RIN transfer as a function of input signal power for three different input pump powers. Fiber length is 500m and $r_p = -100$ dB.

The purpose of Fig. 5 is to show the role of input pump power and the pump depletion due to the input signal power for a fixed fiber length (500 m). Increasing the input signal power depletes the pump power and therefore lowers the RIN transfer. The saturation behavior is also the same as that of Fig. 4. It is worth mentioning that basically Fig. 5 is equivalent to Fig. 1. For example, if one considers a particular curve in Fig. 1 for a given input pump power, say the top curve, its counterpart in Fig. 5 would also be the top curve since both curves are plotted for the same input signal power. Based on Fig. 1, experimentally investigating the nonlinear dynamics of the pump-to-signal RIN transfer, demands the cut-back technique which is normally a destructive approach. To get rid of this issue, one can equivalently perform the experiment for a fixed fiber length, but for various input pump powers instead.

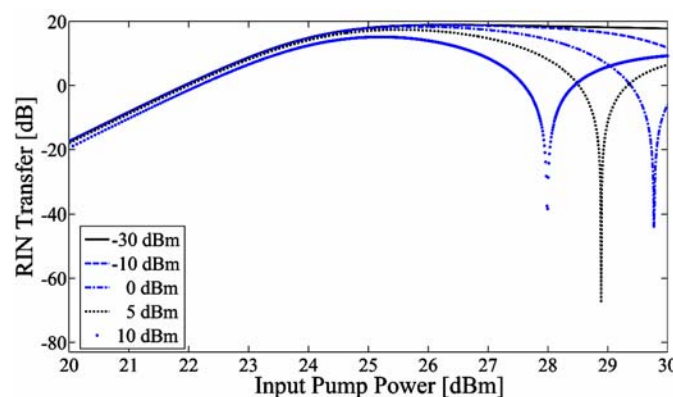


Fig. 5. RIN transfer as a function of input pump power for different input signal powers. Fiber length is 500 m and $r_p = -100$ dB.

b) Comparison with Experimental Results

This part is aimed to verify our model predictions using the comparison between the numerical results and the experimental ones, as well as the available theory in this field [12]. To do this, we compare

our results to those of ref.12. In their work, the same concept as RIN transfer, but with a different definition has been used. RIN magnification factor, which is defined as $\rho = m_s / m_p$, was used to describe the pump-to-signal transfer of low-frequency IM in FOPAs. $m_{p,s}$ is the intensity modulation index of the pump and signal measured at the input and output of the FOPA, respectively. So in this part, to ease the comparison, this definition is used in our calculations as well.

Parameters of the fiber used in this part for the numerical analysis are those of ref.12, i.e., $L = 500$ m, $\gamma = 17 \text{ W}^{-1} \text{ km}^{-1}$ and $S = 0.03 \text{ ps} / (\text{nm}^2 \text{ km})$. We also consider $m_p = 0.1$ and $m_s = 0$ the same as in ref.12. An analytical expression was derived in the mentioned reference which is valid under some approximations including small signal, no pump depletion and no loss. In order to perform the numerical calculations one has to know about the values of input signal power as well as the loss, which has not been mentioned in the above article. To determine these values, the best fit was made in order to match the numerical results with the experimental data of the parametric gain. As it has been shown in Fig. 6 (b), the fit is achieved for $P_s = -30 \text{ dBm}$ and $\alpha = 1.5 \text{ dB/km}$ where there is a very good agreement, especially near the gain peak at which the RIN magnification factor is calculated (Fig. 7). However, as it is shown in Fig. 6 (a), considering $\alpha = 0$ in the numerical model reproduces the analytical results. This shows that the results of our model can match very well with those of analytical whenever the fiber loss is ignored.

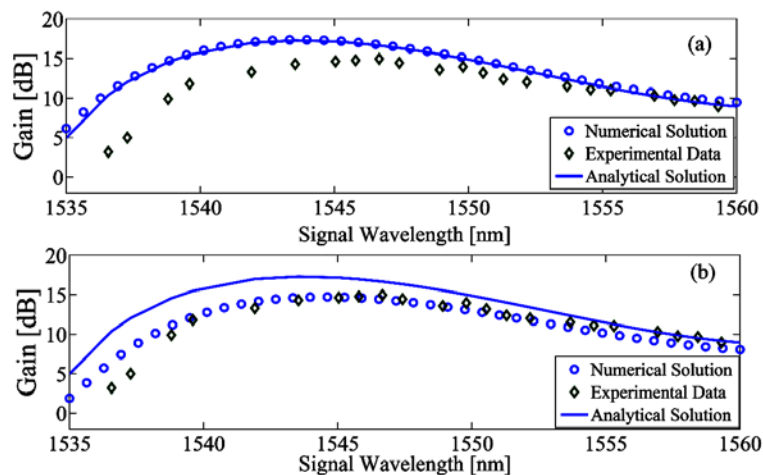


Fig. 6. Experimental parametric gain as well as the analytical and numerical fits. The numerical solution in 6 (a) is obtained for no loss and $P_s = -30 \text{ dBm}$; whereas in 6 (b) the solution is obtained for $\alpha = 1.5 \text{ dB/km}$ and $P_s = -30 \text{ dBm}$. The input pump power and the fiber length are $P_p = 25 \text{ dBm}$, and $L = 500 \text{ m}$, respectively. Experimental data and analytical solution are taken from ref.12

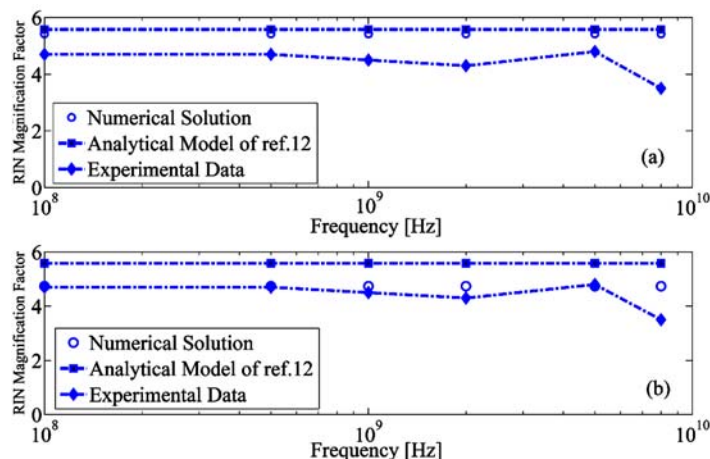


Fig. 7. RIN magnification factor versus RF frequency for a) no loss and $P_s = -30 \text{ dBm}$; b) $\alpha = 1.5 \text{ dB/km}$ and $P_s = -30 \text{ dBm}$. Experimental data are taken from ref.12

In Fig. 7 the RIN magnification factors versus RF frequency for two cases are depicted. In Fig. 7(a) the loss is zero and $P_s = -30$ dBm, whereas in 7 (b) the loss is 1.5dB/ km and $P_s = -30$ dBm. In both cases $P_p = 25$ dBm, and the pump and signal wavelengths are 1562.46 nm and 1544.86 nm, respectively. As we assumed that there is no time-dependent term in the model because of the relatively low IM frequencies, the RIN magnification factor is expected to be constant versus the pump modulation frequency. In other words, the time derivatives of the coupled equations which can be related to the modulation frequency via the Fourier transformation are neglected as a first approximation. Therefore, the equations are independent of the modulation frequency. A frequency-dependent form of the equations can be found in ref. [22]. Figure 7(a) shows that our model is able to reproduce the results of the analytical solution where the signal is very weak and the loss is ignored. On the other hand, if the parameters of the best fit for the gain curve (Fig. 6(b)) are used, a very good agreement between the numerical results and experimental data is achieved (Fig. 7(b)).

In Fig. 8 the dependency of the RIN magnification factor on the signal wavelength has been shown for the two cases as in Fig. 7. The parameters used in Fig. 8(a) and Fig. 8(b) are the same as those of Fig. 7(a) and Fig. 7(b), respectively. Again, a very good agreement is observed when we set $\alpha = 1.5$ dB/km and $P_s = -30$ dBm. The discrepancy between the model and experimental data for the first point on the short-wavelength side is because of the corresponding discrepancy in the gain curve (Fig. 6(b)). Figure 8 gives some interesting results regarding the wide-bandwidth amplification. As it is clear, when the signal wavelength moves towards the gain edge on the short-wavelength side, it acquires more RIN from the pump. The RIN magnification factor can vary by an order of magnitude as we cross the whole bandwidth, such that a signal whose wavelength is located at the gain edge would be very noisy at the FOPA output. These considerations have to be taken into account in optical communication systems, e.g., WDMs [23]. Therefore, it is confirmed that our model can predict the experimental results with a very good accuracy.

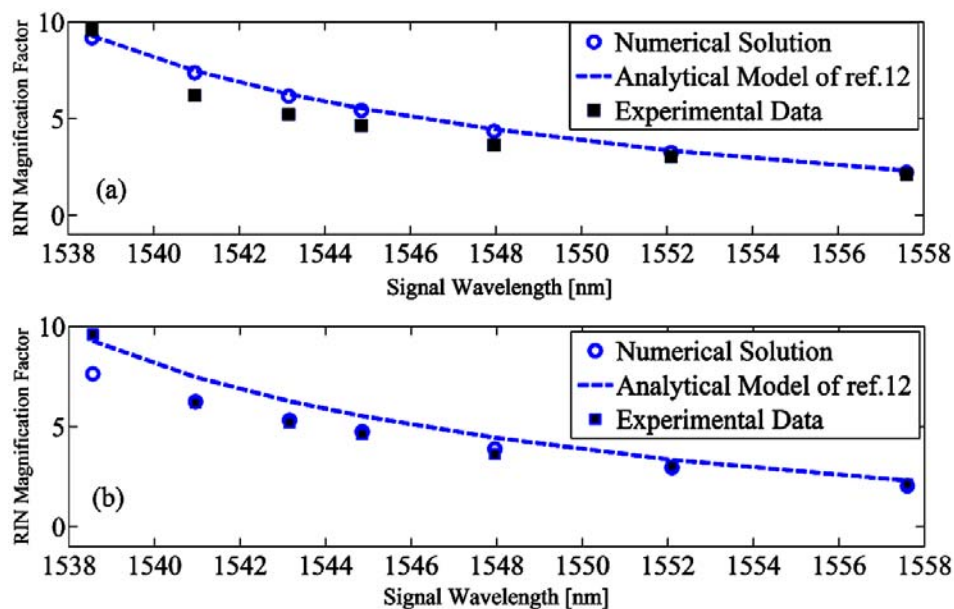


Fig. 8. Wavelength dependence of RIN magnification factor a) no loss and $P_s = -30$ dBm; b) $\alpha = 1.5$ dB/km and $P_s = -30$ dBm. Experimental data are taken from ref.12

Figure 9 shows the evolution of the pump and signal power variations as they propagate along the fiber for various input signal powers. The input pump power and its modulation index are assumed to be 25 dBm and 0.1, respectively.

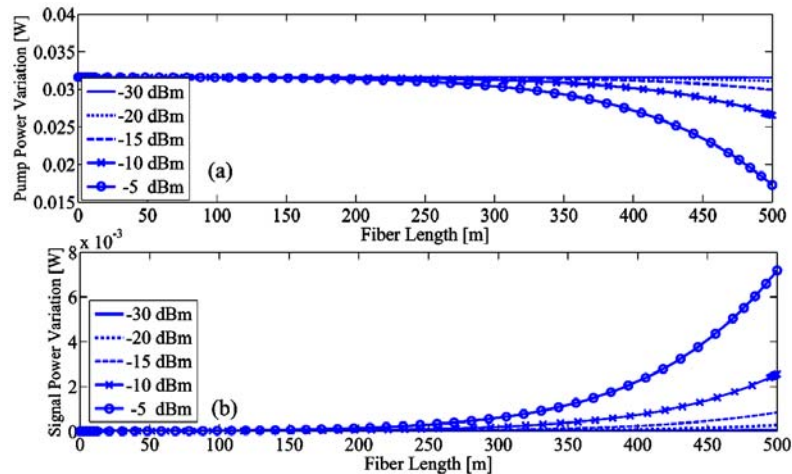


Fig. 9. Evolution of the pump power variation (a) and signal power variation (b) along the fiber for various input signal powers. $P_p = 25$ dBm, $\alpha = 0$, and $m_p = 0.1$

We have also assumed a lossless FOPA. As is seen, for short fiber lengths (shorter than 200 m) the variations remain unchanged. This is because when the fiber is short, the pump does not experience any depletion even though the signal is not so weak. In particular, for a weak signal, less than -20 dBm, both the pump power variation (Fig. 9(a)) and the corresponding signal power variation (Fig. 9(b)) remain unchanged throughout the FOPA. This was firstly established in [12] for the small-signal limit. However, when the input signal power increases, the pump power variation begins to be decreased and the corresponding signal variation begins to be increased so that the energy conservation law among the interacting waves, pump, signal, and idler is maintained. This behavior cannot be predicted by the analytical model since the pump depletion takes place and hence the small-signal limit no longer holds. In fact, Fig. 9 clearly shows how the pump RIN is transferred to the amplified signal and deteriorates it. Therefore, it is confirmed that not only can our model predict the experimental results with a very good accuracy [24], but it also gives more insight, especially when the analytical solutions are not applicable.

4. CONCLUSION

A new numerical model which has been proposed predicts the RIN transfer in single-pump FOPAs when the IM frequencies are low. The model does not suffer from approximations like no loss, no pump depletion and small signals, so it can be well matched to practical conditions. Since the pump is mainly responsible for RIN transfer to the signal, the higher input pump powers lead to higher RIN transfers. On the other hand, for high input signal powers, the greater the pump depletion, and therefore, lower RIN transfers are observed. Near the saturation point where the signal is high enough, the minimum RIN transfer takes place. The numerical results of the model were verified by the available experimental data in the literature and a very good agreement was obtained. The model also matches well with the analytical results where the signal is very weak and the loss is ignored. Moreover, our model can work beyond the small-signal limit which would be the case for some FOPA-based applications such as wavelength converters, regenerators, and amplitude limiters where the analytical model is not applicable. The predictions of the model may have some implications in optical communication systems where the noise is one of the main concerns and clean amplified signals are desirable.

Acknowledgement - The authors would like to thank Karsten Rottwitt, Michel E. Marhic, and Georgios Kalogerakis for helpful discussions and providing some experimental data.

REFERENCES

1. Torounidis, T., Andrekson, P. A. & Olsson, B. E. (2006). Fiber-optical parametric amplifier with 70-dB gain. *IEEE Photon. Technol. Lett.* 18, 1194-1196.
2. Chavez Boggio, J. M., Windmiller, J. R., Knutzen, M., Jiang, R., Bres, C., Alic, N., Stossel, B., Rottwitt, K. & Radic, S. (2008). 730-nm optical parametric conversion from near-to short-wave infrared band. *Opt. Exp.* 16, 5435-5443.
3. Peucheret, C., Lorenzen, M., Seoane, J., Noordegraaf, D., Nielsen, C. V., Nielsen, L. G. & Rottwitt, K. (2009). Amplitude regeneration of RZ-DPSK signals in single pump fiber optic parametric amplifiers. *IEEE Photon. Technol. Lett.* 21, 872-874.
4. Li, J., Hansryd, J., Hedekvist, P. O., Andrekson, P. A. & Knudsen, S. N. (2001). 300-Gb/s eye-diagram measurement by optical sampling using fiber-based parametric amplification. *IEEE Photon. Technol. Lett.* 13, 987-989.
5. Chavez Boggio, J. M., Moro, S., Myslivets, E., Windmiller, J. R., Alic, N. & Radic, S. (2009). 155-nm continuous-wave two-pump parametric amplification. *IEEE Photon. Technol. Lett.* 21, 612-614.
6. Tang, R., Voss, P. L., Lasri, J., Devgan, P. & Kumar, P. (2003). Noise-figure limit of fiber-optical parametric amplifiers and wavelength converters: experimental investigation. *Opt. Lett.* 29, 2372-74.
7. Kylemark, P., Karlsson, M. & Andrekson, P. A. (2006). Gain and wavelength dependence of the noise-figure in fiber optical parametric amplification. *IEEE Photon. Technol. Lett.* 18, 1255-1257.
8. Velanas, P., Bogris, A. & Syvridis, D. (2004). Impact of dispersion fluctuations on the noise properties of fiber optic parametric amplifiers. *J. Lightwave Technol.* 24, 2171-2178.
9. Durécu-Legrand, A., Simonneau, C., Bayart, D., Mussot, A., Sylvestre, T., Lantz, E. & Maillotte, H. (2006). Impact of pump OSNR on noise figure for fiber-optical parametric amplifiers. *IEEE Photon. Technol. Lett.* 17, 1178-1180.
10. Gao, M., Jiang, C., Hu, W., Wang, J. & Ren, H. (2005). The effects of pump noise on noise characteristics of fiber optical parametric amplifiers. *Opt. Commun.* 266, 181-186.
11. Voss, P. L. & Kumar, P. (2004). Raman-noise-induced noise-figure limit for $\chi^{(3)}$ parametric amplifiers. *Opt. Lett.* 29, 445-447.
12. Marhic, M. E., Kalogerakis, G., Wong, K. K.-Y. & Kazovsky, L. G. (2005). Pump-to-signal transfer of low-frequency intensity modulation in fiber optical parametric amplifiers. *J. Lightwave Technol.* 23, 1049-1055.
13. Tong, Z., Bogris, A., Karlsson, M. & Andrekson, P. A. (2010). Raman-induced asymmetric pump noise transfer in fiber-optical parametric amplifiers. *IEEE Photon. Technol. Lett.* 22, 386-388.
14. Tong, Z., Bogris, A., Karlsson, M. & Andrekson, P. A. (2010). Full characterization of the signal and idler noise figure spectra in single-pumped fiber optical parametric amplifiers. *Opt. Exp.* 18, 2884-2893.
15. Kalogerakis, G., Marhic, M. E., Wong, K. K. Y. & Kazovsky, L. G. (2005). Transmission of optical communication signals by distributed parametric amplification. *J. Lightwave Technol.* 23, 2945-2953.
16. Skold, M., Yang, J., Sunnerud, H., Karlsson, M., Oda, S. & Andrekson, P. A. (2008). Constellation diagram analysis of DPSK signal regeneration in a saturated parametric amplifier. *Opt. Exp.* 16, 5974-5982.
17. Matsumoto, M. & Kamio, T. (2008). Nonlinear phase noise reduction of DQPSK signals by a phase-preserving amplitude limiter using four-wave mixing in fiber. *IEEE J. Select. Topics Quantum Electron.* 14, 610-615.
18. Hansryd, J., Andrekson, P. A., Westlund, M., Lie, J. & Hedekvist, P. O. (2002). Fiber-based optical parametric amplifiers and their applications. *IEEE J. Select. Topics Quantum Electron.* 8, 506-520.
19. Agrawal, G. P. (2007). *Nonlinear Fiber Optics*, 4th ed. Academic Press.
20. Zhou, J., Chen, J., Jaouën, Y., Yi, L., Li, X., Petit, H. & Gallion, P. (2007). A new frequency model for pump-to-signal RIN transfer in Brillouin fiber amplifiers. *IEEE Photon. Technol. Lett.* 19, 1049-1055.

21. Inoue, K. & Mukai, T., (2002). Experimental study on noise characteristics of a gain-saturated fiber optical parametric amplifier. *J. Lightwave Technol.* 20, 969-974.
22. Pakarzadeh, H., Rottwitt, K. & Zakery, A. (2009). Frequency dependence of the pump-to-signal RIN transfer in fiber optical parametric amplifiers. *Proceedings of IEEE LEOS 22nd Annual Meeting, Antalya, Turkey, Paper ThV3*, 787-788.
23. Torounidis, T., Sunnerud, H., Hedekvist, P. O. & Andrekson, P. A. (2003). Amplification of WDM signals in fiber-based optical parametric amplifiers. *IEEE Photon. Technol. Lett.* 15, 1061-1063.
24. Pakarzadeh, H. & Zakery, A. (2010). Experimentally confirmed modeling of the pump-to-signal RIN transfer in one-pump fiber optical parametric amplifiers. *14th International Conference "Laser Optics 2010" St. Petersburg, Russia, Paper TuW3*, p06.